Rotational excitation of molecules by slow neutrons

Burke Ritchie
Oak Ridge National Laboratory, Oak Ridge, Tennessee 37830
and Department of Chemistry, University of Alabama,
University, Alabama 35486
(Received 6 March 1981)

Elastic and rotationally inelastic differential cross sections are calculated for slow neutrons incident on gaseous para-H_2^+. This target is chosen as the simplest open-shell molecular system so that the contribution of electromagnetic forces to the scattering can be studied. It is shown that electromagnetic forces are dominant over nuclear forces in $0\to2$ rotational excitation for small-momentum-transfer collisions (low angles at incident energies about twice the $0\to2$ threshold value). For large-momentum-transfer collisions (wide angles at the higher energies or all angles at energies close to threshold) nuclear forces dominate the scattering. The calculations show that low-angle, small-energy-loss experiments would isolate the weak but long-range electromagnetic forces and thus probe target electronic structure.

I. INTRODUCTION

In this paper the electromagnetic contribution to the angular distribution for slow neutrons incident on molecular gaseous "radicals" (open-shell molecules) is studied. Our purpose is to stimulate interest in the measurement of energy-resolved partial cross sections for a particular final rotational state of the molecular target. As an example, the $J=0\to J'=0$, $J=0\to J'=1$, and $J=0\to J'=2$ differential cross sections are calculated for neutrons on H_2^+. The permanent magnetic dipole moments of the target and projectile combine in a dipole-dipole-type interaction. This interaction induces $0\to2$ rotational transitions which dominate this partial cross section for small-momentum-transfer scattering. This dominance occurs because the $0\to J$ nuclear scattering amplitude (normally dominant over the electromagnetic) is proportional to q_{0J}^J for small q_{0J} and $J>0$ (where $\vec{q}_{0J}$ is the momentum-transfer vector). Thus, inherently small electromagnetic contributions are "uncovered" in the low-angle $0\to2$ partial cross section at incident energies well above the threshold value. For an incident energy twice the $0\to2$ threshold at zero scattering angle, the electromagnetic partial cross section is found (Fig. 1) to be about 3 mb and the nuclear partial cross section about one order of magnitude smaller. In contrast, the $0\to0$ partial cross section is about 150 mb under the same conditions and is dominated by the nuclear contribution.

Since about 1967 the theory of molecular rotational excitation by electron impact[1,2] has been heavily studied. The simple first Born results of Gerjuoy and Stein[3] for nonpolar targets were expressed in terms of a few parameters, including the molecular quadrupole moment. Later studies[1,2] were to show, however, that the electron-target interaction is sufficiently strong that the Born theory fails for low-energy electrons except at threshold. In other words, the molecule (M) plus an electron pair is in reality an unbound negative ion M^-, and the electronic structure of M, for which the Born theory provides a partial elucidation, no longer has a simple meaning in the interpretation of experiments.

In contrast, the Born theory for low-energy, nonabsorptive scattering of neutrons by atomic or molecular targets can be expected to be accurate over the entire range of neutron energies owing to the zero (or very short) range of the nuclear forces and the weakness of the electromagnetic forces. For example, total cross-section measurements have been made[4] for neutrons on para- and ortho-H_2 over a range of neutron energies and agreement with the Born theory[5-7] is obtained. As another example, differential cross-section measurements[8] for n, CH_4 and n, NH_3 show satisfactory agreement with the Born theory within approximations made in the evaluation of the Born amplitude. For these targets electromagnetic forces make no contribution to the first Born amplitude due to the orbital and spin symmetry of the electronic states.

In cases in which electromagnetic forces contribute to the first Born amplitude (n,H or n, H_2^+

are the simplest examples), however, nuclear forces are dominant over electromagnetic forces under most circumstances. For example, the magnitude of the nuclear scattering amplitude[5,6] for the n, H pair is about six times larger than the electromagnetic-amplitude magnitude for triplet n, p scattering and about 24 times larger for singlet n,p scattering. On the other hand, it is well known[5,6] that n,H_2 scattering depends strongly on the total antisymmetry of the p,p state which causes the separation into para-H_2 (for even rotational or J states and the singlet spin state) and ortho-H_2 (for odd J states and the triplet spin state). The n,para-H_2 amplitude depends on the combination of n,p singlet, triplet scattering lengths (a_0, a_1, respectively), $3a_1+a_0$. This factor is strongly dependent on the range of the n,p nuclear force since $3a_1 \simeq -a_0$ (giving a vanishing n,para-H_2 elastic cross section) at a range of about 5×10^{-13} cm. On the other hand, the n, ortho-H_2 amplitude contains the factor $a_1 - a_0$ which is very large and insensitive to the range of the small length a_1.

In H_2 the n,e amplitude is zero by cancellation of the contributions for two antiparallel spin electrons. In n, para-$H_2{}^+$, however, the same n, para-p amplitude obtains, and the n,e amplitude exists. For a physically realistic n,p nuclear-force range[6] of

$$r_0 = e^2/mc^2 \simeq 2.82\times 10^{-13} \text{ cm}$$

[for electron charge e, mass m, and velocity of light c], for which (Ref. 6) $a_1 = 5.85\times 10^{-13}$ cm and $a_0 = 23.45\times 10^{-13}$ cm, the constant factors in the n,para-p and n,e amplitudes have a ratio of about four to one. For unpolarized targets there is no interference contribution to the cross section such that n,e scattering is only about $\frac{1}{16}$ of the total. On the other hand, the dependence on $\vec{q}_{0J}$, the momentum-transfer vector for ΔJ even transitions, is quite different for the nuclear and electromagnetic amplitudes such that for small q_{02} collisions, for example, the n,para-p cross section, is reduced to small values relative to the n,e cross section. The n, para-p cross section grows rapidly with increasing scattering angle (increasing q_{02}) and overtakes the n,e cross section by about 25° center-of-mass (c.m.) scattering angle at a c.m. incident energy twice the $\Delta J = 2$ threshold energy (Fig. 1). These calculations suggest the design of low-angle, small-energy-loss experiments on gaseous molecular radicals in order to isolate the weak n,e contributions to the scattering. The n,e cross section for a given ΔJ transition contains a simple dependence on the electron molecular orbital; thus, such experiments would complement x-ray photon-scattering experiments on gaseous targets[9] as a probe of target electronic structure.

For a molecular ion the n spin-orbit interaction with the nuclei[10] never completely vanishes owing to the residual charge at large-n distances. However, its amplitude contains the factor $(m/M)\cot(\theta/2)$ (for neutron mass M and scattering angle θ) such that it is unimportant except for θ less than about 0.5°. For slow neutrons on neutral molecular radicals this interaction is unimportant since it is effectively screened[10] over the entire range of θ.

II. THEORY

In the nonrelativistic limit the n,e interaction[11] is given by the sum of two terms, a spin (n)-orbit(e) and a spin (n)-spin(e) term. In the first Born approximation integration over the c.m.-frame neutron coordinate $\vec{r}_c$ [position of the neutron relative to the midpoint of an assumed constant-magnitude internuclear vector $\vec{R}$ (see Fig. 1)] leads to two scattering amplitudes. The spin-orbit amplitude is given in general form. The spin-spin amplitude is given for an unpaired electron occupying a σ_g orbital. For $0\to J$ rotational transitions these are

$$f_{so}^{(0JM_J m_s m_s')} = \frac{i}{2}\mu_n r_0 \frac{\mu_c}{M}\left[\frac{k_{0J}}{k}\right]^{1/2} \times q_{0J}^{-1}\int d\Omega_q Y^*_{JM_J}(\beta,\gamma) \times\left[\sum_j \langle \psi_j(\vec{r})\chi_{m_s'} \,|\, e^{i\vec{q}_{0J}\cdot\vec{r}}(\vec{\sigma}_n\times\hat{q}_{0J})\cdot(-i\vec{\nabla})\,|\,\psi_j(\vec{r})\chi_{m_s}\rangle\right] Y_{00}(\beta,\gamma)\,, \tag{1a}$$

$$f_{ss}^{(0JM_Jfm_fm_f')} = \frac{1}{4}\mu_n r_0 \frac{\mu_c}{M}\left[\frac{k_{0J}}{k}\right]^{1/2} \times \int d\Omega_q Y^*_{JM_J}(\beta,\gamma) \times \langle \psi(\vec{r})\chi_{fm_f'} | e^{i\vec{q}_{0J}\cdot\vec{r}}[(\vec{\sigma}_n\cdot\hat{q}_{0J})(\vec{\sigma}\cdot\hat{q}_{0J}) - (\vec{\sigma}_n\cdot\vec{\sigma})]\psi(\vec{r})\chi_{fm_f}\rangle Y_{00}(\beta,\gamma)\,, \tag{1b}$$

where $\mu_n = 1.91$ is the magnitude of the neutron magnetic moment, $r_0 = e^2/(mc^2)$ is the classical electron radius, μ_c/M is the collisional reduced to the neutron mass ratio $k_{0J}^2 = k^2 - \Delta\epsilon_{0J}$ for a transition energy $\Delta\epsilon_{0J}$ Ry and c.m.-frame incident energy k^2 Ry, $\vec{q}_{0J} = \vec{k} - \vec{k}_{0J}$ is the momentum-transfer vector in the direction Ω_q (Fig. 2), and $\vec{\sigma}_n$, $\vec{\sigma}$ are the neutron electron Pauli spin vectors (Fig. 2). The rotational eigenfunctions $Y_{JM_J}(\beta,\gamma)$ are defined for an internuclear vector whose orientation relative to $\vec{q}_{0J}$ is specified by Ω_q $[d\Omega_q = \sin\beta d\beta d\gamma]$. χ_{m_s} is a spin eigenfunction of the neutron, and for neutron-electron total angular momentum $\vec{f} = \vec{s}_n + \vec{s}$ ($\vec{s}_i = \frac{1}{2}\vec{\sigma}_i$), χ_{fm_f} is an eigenfunction of f^2 (and of s_n^2, s^2, and $\vec{s}_n\cdot\vec{s}$).

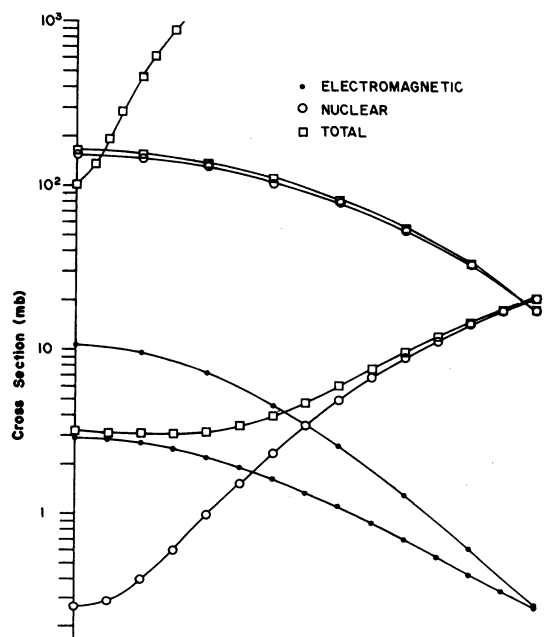

FIG. 1. All energetically allowed partial cross sections for a c.m. incident energy equal to twice the $\Delta J = 2$ threshold value. Between about 5 and 25°. c.m. scattering angles, the cross sections from top to bottom are the following: $0 \rightarrow 1$ total; for $0 \rightarrow 0$, total, nuclear, and electromagnetic; for $0 \rightarrow 2$, total, electromagnetic, and nuclear.

The spin-orbit amplitude is zero for the H_2^+ target. It deserves further comment, however. In Eq. (1a) performance of the summation over j (occupied orbitals), integration of each term by parts, and use of the result $(\vec{\sigma}_n \times \vec{q}_{0J})\cdot\vec{q}_{0J} = 0$ show that the spin-orbit amplitude vanishes by cancellation of $|m_l|$ and $-|m_l|$ contributions provided the target symmetry is high enough that m_l orbital components give equal matrix-element contributions for $\pm m_l$ values. Individual $m_l = 0$ contributions are zero. It is usually assumed that the spin-orbit amplitude is zero for all closed-shell targets. This assumption fails for chiral targets,[12–14] for example. Electromagnetic amplitudes such as those given by Eqs. (1) are presented in the context of other applications in the literature[15]; however, a detailed theory for specific gaseous targets appears not to be available.

For an unpolarized target gas, the electromagnetic cross section is given by the squared moduli of Eq. (1b), summed over $f = 0$ (singlet scattering), over $m_f m_f'$ for $f = 1$ (triplet scattering), and over M_J. This result is divided by four, the total spin degeneracy in the incident channel. The operator in square brackets in Eq. (1b) is diagonal in $f = 0$ and 1. The second term is diagonal in $m_f m_f'$ for $f = 1$; the first term, however, is not. The 3 matrix formed by the $m_f m_f'$ elements for $f = 1$ is presented in the Appendix.

As in the case of electron impact,[3] the Born theory is expressed in terms of the orientation of a rotating molecule-fixed frame (Fig. 2) relative to the momentum-transfer vector $\vec{q}_{0J}$ whose direction is fixed in a laboratory frame for a given scattering angle. In Eq. (1b) the scalar products in the first square-bracket term are evaluated using the Pauli spin matrices[16] to represent the spin vectors. For the neutron, the result is

$$\hat{q}_{0J}\cdot\vec{\sigma}_n = \begin{bmatrix} \cos\beta & \sin\beta e^{-i\gamma} \\ \sin\beta e^{i\gamma} & -\cos\beta \end{bmatrix}_n , \tag{2}$$

where the subscript on the matrix indicates that its basis vectors are the neutron spin eigenfunctions

$$\chi_{1/2}=\begin{bmatrix}1\\0\end{bmatrix}$$

and

$$\chi_{-1/2}=\begin{bmatrix}0\\1\end{bmatrix}.$$

Similarly, Eq. (2) without the n subscript is the matrix representation of the scalar product $\hat{q}_{0J}\cdot\sigma$ whose basis vectors are the electron-spin eigenfunctions

$$\alpha_e=\begin{bmatrix}1\\0\end{bmatrix}$$

and

$$\beta_e=\begin{bmatrix}0\\1\end{bmatrix}.$$

All basis vectors depend on spin quantization along the rotating molecular axis (Fig. 2). The geometric interpretation of Eq. (2) for the Cartesian components of either spin in the rotating frame is given by Fig. 2. The matrix elements for the $f=1$ state (see the Appendix) are linear combinations of $Y_{00}(\beta,\gamma)$ and $Y_{2M}(\beta,\gamma)$ formed from the product of two spin dipoles. The latter spherical harmonic is the source of the small-momentum-transfer electromagnetic dominance stated above since it causes $0\rightarrow2$ rotational transitions to occur for the leading, spherically symmetric contribution to the orbital form factor $\langle\psi(\vec{r})\,|\,e^{i\vec{q}_{0J}\cdot\vec{r}}\,|\,\psi(\vec{r})\rangle$ of Eq. (1b). All other transition amplitudes inclusive of the nuclear (Ref. 5 and below) depend on q_{0J}^J for small q_{0J}. Thus, the spin dipole-dipole contributions to the inherently small electromagnetic amplitudes are "uncovered" when the large nuclear amplitudes become small as q_{0J}^J (see Fig. 1). [Alternatively, the electromagnetic cross section evidently can be derived starting with Eq. (5.9) in Ref. 15.]

The final result for the electromagnetic differential cross section is

$$\frac{d\sigma_e^{(OJ)}}{d\Omega}=\frac{(\mu_n r_0)^2}{54}\frac{k_{OJ}}{k}(2J+1)(F_{J2}+2F_J)\,, \tag{3a}$$

$$F_J=\sum_{ll'\lambda\lambda'}(2l+1)^{1/2}(2l'+1)^{1/2}(2\lambda+1)^{1/2}(2\lambda'+1)^{1/2}\begin{bmatrix}l' & J & l\\0&0&0\end{bmatrix}^2\begin{bmatrix}\lambda' & J & \lambda\\0&0&0\end{bmatrix}^2 R_{\lambda J\lambda'}R_{lJl'}\,, \tag{3b}$$

$$F_{J2}=\sum_{ll'\lambda\lambda'n}(2l+1)^{1/2}(2l'+1)^{1/2}(2\lambda+1)^{1/2}(2\lambda'+1)^{1/2}(2n+1)\begin{bmatrix}J & 2 & n\\0&0&0\end{bmatrix}^2 \times\begin{bmatrix}l' & n & l\\0&0&0\end{bmatrix}^2\begin{bmatrix}\lambda' & n & \lambda\\0&0&0\end{bmatrix}^2 R_{\lambda n\lambda'}R_{lnl'}\,, \tag{3c}$$

$$R_{lsl'}=\int_0^\infty dr\,\psi_{l'0}(r)j_s(q_{0J}r)\psi_{l0}(r)\,. \tag{3d}$$

Equations (3) depend on the use of a single-center expansion[17] for the orbital

$$\psi(\vec{r})=\sum_l\frac{\psi_{l0}(r)}{r}Y_{l0}(\theta_r,\phi_r) \tag{4}$$

about the midpoint of $\vec{R}$ (Fig. 1). This expansion is known to be reasonably accurate in the description of e,H_2^+ elastic scattering.[17,18]

For ΔJ even transitions the total cross section is the sum of nuclear and electromagnetic cross sections

$$\frac{d\sigma^{(OJ)}}{d\Omega}=\frac{4}{9}\frac{k_{OJ}}{k}(2J+1)(3a_1+a_0)^2 j_J^2(q_{0J}R/2)+\frac{d\sigma_e^{(OJ)}}{d\Omega}\,. \tag{5}$$

For ΔJ odd transitions only nuclear scattering

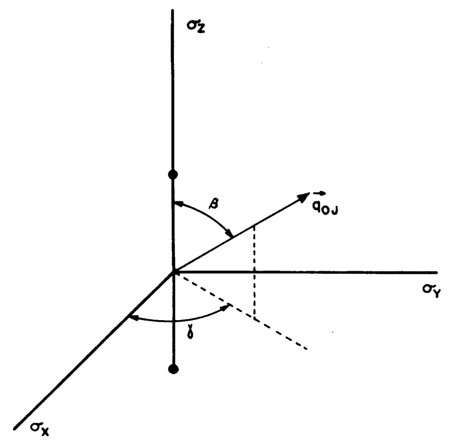

FIG. 2. Orientation of the rotating molecule-fixed frame relative to the momentum-transfer vector $\vec{q}_{0J}$ (whose direction is fixed in the laboratory frame). The axes of the rotating frame are labeled by the Cartesian components of the bound-electron spin vector $\vec{\sigma}$.

occurs,

$$\frac{d\sigma^{(0J)}}{d\Omega_o}=\frac{4}{3}\,\frac{k_{0J}}{k}(2J+1)$$

$$\times(a_1-a_0)^2 j_J^2(q_{0J}R/2)\,. \quad (6)$$

$R=2a_0$ is the interproton distance. Scattering into Ω is determined by the momentum transfer

$$q_{0J}=(k^2+k_{0J}^2-2kk_{0J}\cos\theta)^{1/2}\,. \quad (7)$$

III. RESULTS AND CONCLUSIONS

All energetically allowed partial cross sections for a c.m. incident energy equal to twice $\Delta\epsilon_{0J}=0.021\,591$ eV (Ref. 19) are plotted in Fig. 1. For c.m. scattering angles between about 5 and 25 deg the curves from top to bottom are the $0\to1$ (top), $0\to0$ (next three), and $0\to2$ (bottom three) partial cross sections. The electromagnetic and nuclear contributions to each partial cross section are plotted separately for the $0\to0$ and $0\to2$ channels. It is clear that electromagnetic contributions are not significant except at low angles in the $0\to2$ channel, as stated previously. For $0\to2$ transitions the electromagnetic contribution is seen to be dominant for c.m. angles as wide as 15°. At about 25°. (at the crossing point) the electromagnetic and nuclear contributions are equal. Beyond about 40 deg the nuclear contribution is dominant.

These calculations suggest the design of low-angle, energy-resolved neutron beam experiments on target gases such as O_2 and NO. The simple dependence of the electromagnetic amplitude on the orbital form factor of the unpaired electron [Eq. (1b)] provides an experimental test of molecular-orbital theory for such open-shell targets. For NO the spin-orbit amplitude will also contribute to electromagnetic scattering.

ACKNOWLEDGMENTS

This research was sponsored by the Office of Health and Environmental Research, U.S. Department of Energy under Contract No. W-7405-eng-26 with the Union Carbide Corporation. Acknowledgment is made to the Donors of the Petroleum Research Fund, administered by the American Chemical Society, for the partial support of this research. The author would also like to thank M. E. Riley for his expert advice on the evaluation of the matrix elements in Eq. (1a).

APPENDIX

Use of n,e states of total angular momentum $f=1$ leads to the following 3 matrix when the operator (O) in square brackets of Eq. (1b) is evaluated for the elements $(m_f',\,O\,m_f)$,

$$O=\begin{pmatrix} -\frac{2}{3}[1-P_2(\cos\beta)] & \frac{\sqrt{2}}{3}P_2^1(\cos\beta)e^{-i\gamma} & \frac{1}{3}P_2^2(\cos\beta)e^{-2i\gamma} \\ \frac{\sqrt{2}}{3}P_2^1(\cos\beta)e^{i\gamma} & -\frac{2}{3}[1+2P_2(\cos\beta)] & -\frac{\sqrt{2}}{3}P_2^1(\cos\beta)e^{-i\gamma} \\ \frac{1}{3}P_2^2(\cos\beta)e^{2i\gamma} & -\frac{\sqrt{2}}{3}P_2^1(\cos\beta)e^{i\gamma} & -\frac{2}{3}[1-P_2(\cos\beta)] \end{pmatrix}.$$

The 1 matrix for $f=0$ has the value 2. Each element of the 1 and 3 matrices is multiplied by

$$Y_{JM_J}^*(\beta,\gamma)\langle\psi(\vec{r})\,|\,e^{i\vec{q}_{0J}\cdot\vec{r}}\,|\,\psi(\vec{r})\rangle Y_{00}(\beta,\gamma)$$

and the result is integrated over Ω_q. The sum of the squared moduli of these results, divided by 4 and multiplied by $\frac{1}{16}(\mu_n r_0\mu_c/M)^2\,k_{0J}/k$, leads to Eqs. (3).

[1]D. E. Golden, N. F. Lane, A. Temkin, and E. Gerjuoy, Rev. Mod. Phys. 43, 642 (1971).
[2]N. F. Lane, Rev. Mod. Phys. 52, 29 (1980).
[3]E. Gerjuoy and S. Stein, Phys. Rev. 97, 1671 (1955); 98, 1848 (1955).
[4]G. L. Squires and A. T. Stewart, Proc. R. Soc. London, Ser. A 230, 19 (1955).
[5]J. Schwinger and E. Teller, Phys. Rev. 52, 286 (1937).
[6]M. Hamermesh and J. Schwinger, Phys. Rev. 71, 678 (1947).
[7]J. A. Young and J. U. Koppel, Nukleonik 8, 40 (1966).
[8]F. J. Webb, Proc. Phys. Soc. London 92, 912 (1967).
[9]G. E. Ice, M. H. Chen, and B. Crasemann, Phys. Rev. A 17, 650 (1978).
[10]J. Schwinger, Phys. Rev. 73, 407 (1948).
[11]N. F. Mott and H. S. W. Massey, *Theory of Atomic Collisions,* 3rd ed. (Clarendon, Oxford, 1965), pp. 786–788.
[12]B. Ritchie, Phys. Rev. A 13, 1411 (1976).
[13]B. Ritchie, Phys. Rev. A 20, 1915 (1979).
[14]B. Ritchie (unpublished).
[15]W. Marshall and S. W. Lovesey, *Theory of Thermal Neutron Scattering* (Clarendon, Oxford, 1971), Chap. 5.
[16]H. A. Bethe and E. E. Salpeter, *Quantum Mechanics of One- and Two-Electron Atoms* (Springer, Berlin, 1957), p. 48.
[17]A. Temkin and K. V. Vasavada, Phys. Rev. 160, 109 (1967).
[18]W. D. Robb and L. A. Collins, Phys. Rev. A 22, 2474 (1980).
[19]S. Cohen, J. R. Hiskes, and R. J. Riddell, Phys. Rev. 119, 1025 (1960).